Ovchinnikov M.Y., **Roldugin D.S.**, **Penkov V.I.**

Magnetically actuated dual-spin satellite periodical motion during in-orbit attitude maneuvers

M.Yu. Ovchinnikov, D.S. Roldugin, V.I. Penkov

Magnetically actuated dual-spin satellite periodical motion during the in-orbit attitude maneuver

Овчинников М.Ю., Ролдугин Д.С., Пеньков В.И.

Периодические движения спутника с магнитным управлением и маховиком при повороте в плоскости орбиты

Рассматривается спутник, оснащенный магнитной системой ориентации и тангажным маховиком. Исследуется алгоритм ориентации спутника в плоскости орбиты при движении вблизи требуемой ориентации. Найдены амплитуды плоских и пространственных периодических движений, показывающие точность ориентации. Проведено исследование устойчивости, численное моделирование.

Ключевые слова: магнитная система ориентации, тангажный маховик, периодические решения

Mikhail Ovchinnikov, Dmitry Roldugin, Vladimir Penkov

Magnetically actuated dual-spin satellite periodical motion during the in-orbit attitude maneuvers

Attitude motion of a satellite equipped with a single flywheel and an active magnetic attitude control system is considered. Control system ensures necessary attitude in orbital plane. Periodic solutions amplitudes are found for planar and spatial motion. Stability and numerical analysis is carried out.

Key words: magnetic attitude control system, flywheel, dual spin, periodic motion

Contents

Introduction

Dual-spin satellite with the active magnetic attitude control system is considered. Flywheel with large angular momentum ensures orbital attitude with the flywheel pointing along the normal to the orbit. The magnetic attitude control system provides asymptotical stability for this motion and rotation in the orbital plane. This paper follows [1,2] where transient motion was considered mainly. Attitude in the vicinity of necessary position was covered briefly. This paper enhances the suggested magnetic control law that ensures necessary rotation in the orbital plane. In-plane and spatial periodical motions are found. This provides necessary insight into the attitude accuracy.

1.   Problem statement

The satellite is considered to be a rigid body. It moves along the circular orbit in the dipole geomagnetic field. The satellite is equipped with a flywheel (constant rotation wheel) and three mutually orthogonal magnetorquers. Current attitude is thought to be available. Two reference frames are used:

- orbital frame $OX_1X_2X_3$ has its center at the satellite's center of mass O. OX_3 axis is directed along the radius vector, OX_2 coincides with the orbital normal, OX_1 is directed along the translational orbital velocity;

- bound frame $Ox_1x_2x_3$ has its axis directed along the principal axes of inertia of the satellite.

Satellite attitude with respect to the orbital frame is given by angles α, β, γ (rotation sequence 2-3-1) and angular velocity components. Quaternion is used instead of angles for numerical simulations. Transition matrix is

$$\mathbf{A} = \begin{pmatrix} \cos\alpha\cos\beta & \sin\beta & -\sin\alpha\cos\beta \\ -\cos\alpha\sin\beta\cos\gamma + \sin\alpha\sin\gamma & \cos\beta\cos\gamma & \sin\alpha\sin\beta\cos\gamma + \cos\alpha\sin\gamma \\ \sin\alpha\cos\gamma + \cos\alpha\sin\beta\sin\gamma & -\cos\beta\sin\gamma & -\sin\alpha\sin\beta\sin\gamma + \cos\alpha\cos\gamma \end{pmatrix}. \qquad (1.1)$$

Dynamical equations of the satellite with inertia tensor $\mathbf{J} = diag(A, B, C)$ are

$$\mathbf{J}\frac{d\mathbf{\omega}}{dt} + \mathbf{\omega} \times \mathbf{J}\mathbf{\omega} + \mathbf{\omega} \times \mathbf{h} = \mathbf{M}_{gr} + \mathbf{M}_{ctrl} \qquad (1.2)$$

where $\mathbf{h} = (0, h, 0)$ is the flywheel angular momentum, $\mathbf{M}_{gr}$ and $\mathbf{M}_{ctrl}$ are the gravitational and control torques. Kinematics is described as

$$\frac{d\alpha}{dt} = \frac{1}{\cos\beta}\left(\Omega_2\cos\gamma - \Omega_3\sin\gamma\right),$$

$$\frac{d\beta}{dt} = \Omega_2\sin\gamma + \Omega_3\cos\gamma, \tag{1.3}$$

$$\frac{d\gamma}{dt} = \Omega_1 - \text{tg}\,\beta\left(\Omega_2\cos\gamma - \Omega_3\sin\gamma\right).$$

Absolute angular velocity $\boldsymbol{\omega}$ is tied with the relative one $\boldsymbol{\Omega}$ through the relation

$$\boldsymbol{\omega} = \boldsymbol{\Omega} + \mathbf{A}\boldsymbol{\omega}_{orb}$$

where $\boldsymbol{\omega}_{orb} = (0, \omega_0, 0)$ is the orbital reference frame angular velocity. The geomagnetic induction vector is modelled using the direct dipole [3]. The exact expression is

$$\mathbf{B} = B_0\left(\cos u \sin i,\ \cos i,\ -2\sin u \sin i\right) = B_0\left(B_1, B_2, B_3\right)$$

where i is the orbit inclination, u is the argument of latitude.

Transient motion was considered in [1,2]. Motion in the vicinity of necessary attitude was briefly discussed. Gravitationally stable position and rotation in the orbital plane were covered. The latter was ensured with the control

$$\mathbf{M}_r = \left(0, k_r\varepsilon\sin\left(\alpha_d - \alpha\right), -k_r\varepsilon\sin\left(\alpha_d - \alpha\right)\frac{B_{2x}}{B_{3x}}\right) \tag{1.4}$$

where k_r is a positive dimensionless constant, $\varepsilon = kB_0^2/C\omega_0$, B_{ix} stands for the i-th component of the geomagnetic induction vector in the bound frame. The attitude accuracy estimation and numerical simulation cases were provided. However control (1.4) suffers from singularity. This overburdens control scheme with auxiliary conditions in order to eliminate situations where B_{3x} is close to zero. Consider similar control

$$\mathbf{M}_r = \left(0, k_r\varepsilon\sin\left(\alpha_d - \alpha\right)B_{3x}^2, -k_r\varepsilon\sin\left(\alpha_d - \alpha\right)B_{2x}B_{3x}\right). \tag{1.5}$$

It is implemented with the first magnetorquer. Third magnetorquer provides control

$$\mathbf{M}_r = \left(-k_r\varepsilon\sin\left(\alpha_d - \alpha\right)B_{1x}B_{2x}, k_r\varepsilon\sin\left(\alpha_d - \alpha\right)B_{1x}^2, 0\right)$$

that won't be covered here.

Control (1.5) influence is studied using the linearized equations of motion. Assume that after the transient motion $\beta, \gamma \sim 0$, $\Omega_i \sim 0$. Linearized in the vicinity of this motion equations are

$$\ddot{\gamma} + (1 - \theta_A)\dot{\beta} + \theta_A\gamma = -3\lambda_A\left(\beta\sin\alpha\cos\alpha + \gamma\cos^2\alpha\right) + \varepsilon C/A\bar{M}_1,$$

$$\ddot{\alpha} = 3\lambda_B\sin\alpha\cos\alpha + \varepsilon C/B\bar{M}_2, \tag{1.6}$$

$$\ddot{\beta} + (\theta_C - 1)\dot{\gamma} + \theta_C\beta = -3\lambda_C\left(\gamma\sin\alpha\cos\alpha + \beta\sin^2\alpha\right) + \varepsilon\bar{M}_3$$

where $\lambda_A = \dfrac{B-C}{A}$, $\lambda_B = \dfrac{C-A}{B}$, $\lambda_C = \dfrac{B-A}{C}$, $h_A = \dfrac{h}{A\omega_0}$, $h_C = \dfrac{h}{C\omega_0}$, $\theta_A = h_A + \lambda_A$,

$\theta_C = h_C + \lambda_C$, $\bar{M}_i$ are the dimensionless torque components, derivatives are with respect to the argument of latitude. Control (1.5) is supplemented with the damping dipole moment $\mathbf{m} = k\left(\mathbf{\Omega}\times\mathbf{B}\right)$. The linearized damping control torque is

$$\mathbf{M} = k\omega_0 B_0^2 \begin{pmatrix} \dot{\beta}B_{1x}B_{3x} - \dot{\gamma}\left(B_{2x}^2 + B_{3x}^2\right) + \dot{\alpha}B_{1x}B_{2x} \\ \dot{\gamma}B_{1x}B_{2x} - \dot{\alpha}\left(B_{1x}^2 + B_{3x}^2\right) + \dot{\beta}B_{2x}B_{3x} \\ \dot{\alpha}B_{2x}B_{3x} - \dot{\beta}\left(B_{2x}^2 + B_{1x}^2\right) + \dot{\gamma}B_{1x}B_{3x} \end{pmatrix}. \tag{1.7}$$

Dimensional parameter k governs overall magnetic control torque value. Dimensionless parameter k_r provides the positional part contribution.

2. Planar motion on polar orbit

Periodical planar motion

Polar orbit allows separate equations for the planar in-plane motion (angle α). Spatial out-of-plane motion allows the solution $\beta = \gamma = 0$. This is due to the relation (1.7) that provides $B_{2x} = 0$. In-plane motion equation is

$$\ddot{\alpha} = 3\lambda_B\sin\alpha\cos\alpha + \varepsilon C/B\left[k_r\sin(\alpha_d - \alpha)(\cos u\sin\alpha - 2\sin u\cos\alpha)^2 - (1 + 3\sin^2 u)\dot{\alpha}\right]. \tag{2.1}$$

Gravitational torque shifts the equilibrium position towards $\alpha = 0$ (we specify $B > C$). Periodical variations of the geomagnetic induction vector lead to periodical oscillations near this new equilibrium position. Let's estimate the displacement of the equilibrium position in the orbital plane due to the gravitational torque. Assume both gravitational and control magnetic torques to be small ($\lambda_B \ll 1$, $\varepsilon \ll 1$). Small control torque is often ensured by the relatively weak magnetorquers installed on small satellites. Gravitational torque smallness may seem non-natural. However there is no sense in magnetic control if gravitation prevails over it. Clearly the following analysis makes sense only for the proper satellite arrangement: it should not be notably oblate or stretched. Taking into account discussed assumption equations (2.1) may be averaged over the argument of latitude,

$$\ddot{\alpha} = m\mu\sin\alpha\cos\alpha + \mu k_r\sin(\alpha_d - \alpha)\left(1/2\sin^2\alpha + 2\cos^2\alpha\right) - 5/2\mu\dot{\alpha} \tag{2.2}$$

where $\mu = \varepsilon C/B \ll 1$ is a small parameter, parameter $m = \lambda/\mu = 3\lambda_B/\mu = O(1)$ provides the relation between typical values of the gravitational and control magnetic torques. New variable $\rho = \alpha - \alpha_d$ is introduced. It describes the satellite deviation from the necessary attitude. Trigonometric functions in (2.2) are decomposed to the series up to the second order of ρ (angle ρ is not small for large m). New equilibrium position is governed by

$$c_2\rho^2 + c_1\rho + c_0 = 0$$

where

$$c_2 = \mu\sin\alpha_d\cos\alpha_d(3k_r - 2m),$$

$$c_1 = m\mu(\cos^2\alpha_d - \sin^2\alpha_d) - k_r\mu(1/2\sin^2\alpha_d + 2\cos^2\alpha_d),$$

$$c_0 = m\mu\sin\alpha_d\cos\alpha_d.$$

Specific satellite arrangement ($B > C$) provides the equilibrium position

$$\rho_0 = \left(-c_1 - \sqrt{c_1^2 - 4c_0c_2}\right)\Big/2c_2. \tag{2.3}$$

Note that $c_2 \neq 0$ for realistic satellite parameters. Consider the satellite with parameters $A = 1.5$, $B = 1.7$, $C = 1.3$ kg·m²/s, $k = 5/3 \cdot 10^6$ N·m·s/T², $k_r = 3$, orbit altitude 1000 km. Typical control and gravitational torque values are $\mu \approx 0.37$ and $\lambda = 3\lambda_B \approx -0.35$. If necessary attitude in orbital plane is $\alpha_d = 40°$ then new equilibrium position becomes $\alpha' = \alpha_d + \rho_0 \approx 34.5°$. Despite close values of control and gravitational torques equilibrium position deviation is small. Linearization of equation (2.1) near α' (substitution $\alpha = \alpha' + x$) yields

$$\ddot{x} = \mu\left[m(b^2 - a^2) - dk_r(a\cos u - 2b\sin u)^2 - 2ck_r(a\cos u - 2b\sin u)(b\cos u + 2a\sin u)\right]x +$$

$$+ \mu\left[mab - ck_r(a\cos u - 2b\sin u)^2\right] - \mu(1 + 3\sin^2 u)\dot{x}$$

where $a = \sin\alpha'$, $b = \cos\alpha'$, $c = \sin\rho_0$, $d = \cos\rho_0$. This equation has the form

$$\ddot{x} = \mu\left[f_0(u) + f_1(u)x + f_2(u)\dot{x}\right]$$

where

$$f_i(u) = a_i + b_i\cos 2u + c_i\sin 2u,$$

$$a_1 = m(b^2 - a^2) - dk_r(2b^2 + 1/2a^2) + 3ck_rab, \quad a_0 = mab - ck_r(2b^2 + 1/2a^2), \quad a_2 = -5/2,$$

$$b_1 = dk_r(2b^2 - 1/2a^2) - 5ck_rab, \quad b_0 = ck_r(2b^2 - 1/2a^2), \quad b_2 = 3/2,$$

$$c_1 = 2dk_rab + 2ck_r(b^2 - a^2), \quad c_0 = 2abck_r, \quad c_2 = 0.$$

Finally linearized equation may be written as

$$\dot{\mathbf{y}} = \mathbf{A}(u)\mathbf{y} + \mathbf{g}(u) \qquad\qquad (2.4)$$

where

$$\mathbf{y} = (x, \dot{x}),$$

$$\mathbf{A}(u) = \begin{pmatrix} 0 & 1 \\ \mu f_1(u) & \mu f_2(u) \end{pmatrix},$$

$$\mathbf{g}(u) = (0, \mu f_0(0)).$$

The amplitudes of π-periodical solutions of (2.4) can be found numerically. Their dependence on the values of control and gravitational torques is of particular interest.
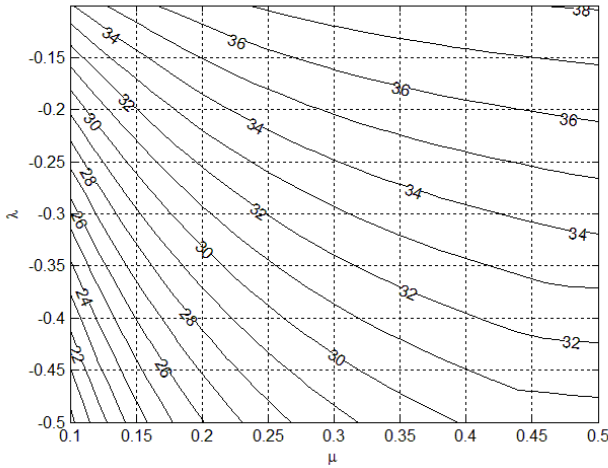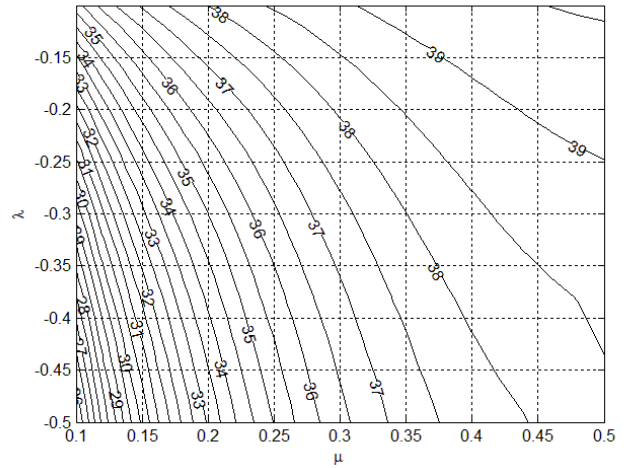

Fig. 1. Minimum angle α Fig. 2. Maximum angle α

Fig. 1 and 2 provide the amplitude calculation results. These are minimum and maximum values of the angle $\alpha_0 = \alpha_d + \rho_0 + x$. Each pair λ, μ provides the equilibrium displacement ρ_0 according to (2.3). This is followed by the periodical solution of equations (2.4). All satellite parameters are retained from the previous example. As the control torque value (parameter μ) increases the amplitude rises. The satellite is closer to the necessary attitude given by $\alpha_d = 40°$. As the gravitational torque (parameter λ) rises the amplitude falls. The satellite is closer to the gravitationally stable equilibrium position $\alpha = 0$. Specific example considered above provides approximate values for α in range 32.58°-38°. Numerical simulation (Fig. 3) of equation (2.1) yields 32.6°-38°.
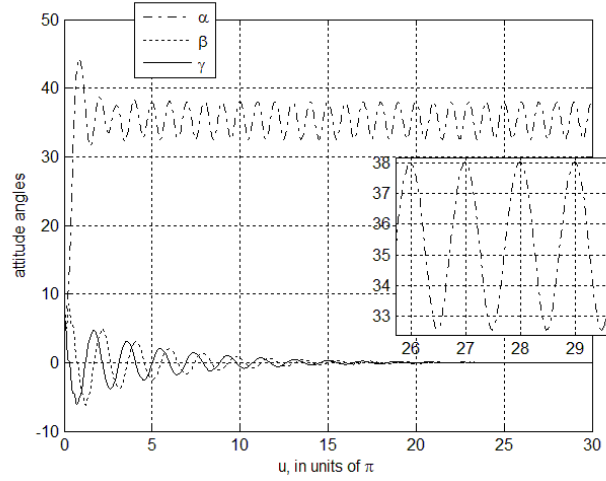
Fig. 3. Numerical simulation of planar motion

Initial conditions of periodical solutions are found along with amplitudes. This information is not used in numerical simulation. Fig. 3 was obtained with initial conditions 0.1 for each variable. Given time the motion tends to the provided periodical solution for α and $\beta = \gamma = 0$. This hints at the asymptotical stability of the found periodical motion.

Stability of the planar periodical motion

Planar periodical solutions may be used [4] to construct spatial periodical motion on a circumpolar orbit. Planar periodical solution $\alpha = \alpha_d + \rho_0 + x$, $\beta = \gamma = 0$ (and corresponding angular velocity rates ω_2, ω_3, ω_1) may be used as a generating solution for equations (1.6) if it is asymptotically stable. In this case the planar motion found earlier becomes the only possible periodical solution on the polar orbit. Hence there exists only one spatial periodical solution on a circumpolar orbit for equations (1.6). It transforms into the planar one as inclination tends to $\pi/2$.

Stability of the planar polar periodical solution is analyzed using the equations in variations. Let «Δ» denote the variation of $\mathbf{x} = (\omega_1, \omega_2, \omega_3, \alpha, \beta, \gamma)$. Then the equations in variations for (1.6) that correspond to the planar solution are

$$\Delta\dot{\mathbf{x}} = \mathbf{A}(u)\Delta\mathbf{x}, \tag{2.5}$$

$$\mathbf{A} = \mathbf{A}_{damp} + \mathbf{A}_{pos} + \mathbf{A}_{kin} + \mathbf{A}_{grav-gir}.$$

Damping control part provides matrix

$$\mathbf{A}_{damp} = \begin{pmatrix} -\varepsilon C/A\,f_1^2 & 0 & -\varepsilon C/A\,f_1 f_2 & 0 & -\varepsilon C/A\,\omega_{20}\,f_2^2 & -\varepsilon C/A\,\omega_{20}\,f_1 f_2 \\ 0 & -\mu(1+3\sin^2 u) & 0 & 0 & 0 & 0 \\ -\varepsilon f_1 f_2 & 0 & -\varepsilon f_2^2 & 0 & \varepsilon\omega_{20}\,f_1 f_2 & \varepsilon\omega_{20}\,f_1^2 \\ & & & 0_{3x6} & & \end{pmatrix},$$

$$f_1 = 2\cos\alpha_0 \sin u - \sin\alpha_0 \cos u,$$
$$f_2 = 2\sin\alpha_0 \sin u + \cos\alpha_0 \cos u.$$

Positional control part yields

$$\mathbf{A}_{pos} = k_r \begin{pmatrix} & 0 & 0 & 0 \\ 0_{3x3} & \mu g_1 & 0 & 0 \\ & 0 & -\varepsilon g_2 f_1 f_2 & -\varepsilon g_2 f_1^2 \\ 0_{3x3} & & 0_{3x3} & \end{pmatrix},$$

$$g_1 = 2\sin(\alpha_0 - \alpha_d)\left[1/2\cos(\alpha_0 + u) - 3/2\cos(\alpha_0 - u)\right] \times \left[3/2\sin(\alpha_0 - u) - 1/2\sin(\alpha_0 + u)\right] -$$
$$- \cos(\alpha_0 - \alpha_d)\left[3/2\sin(\alpha_0 - u) - 1/2\sin(\alpha_0 + u)\right]^2,$$
$$g_2 = \cos\alpha_0 \sin\alpha_d - \cos\alpha_d \sin\alpha_0.$$

Kinematics lead to

$$\mathbf{A}_{kin} = \begin{pmatrix} 0_{3x3} & & 0_{3x3} \\ 0 & 1 & 0 & \\ 0 & 0 & 1 & 0_{3x3} \\ 1 & 0 & 0 & \end{pmatrix}.$$

Gravitational and gyroscopic torques correspond to the matrix

$$\mathbf{A}_{grav-gir} = \begin{pmatrix} 0 & 0 & \theta_A - 1 & 0 & -3\lambda_A \sin\alpha_0 \cos\alpha_0 & -3\lambda_A \cos^2\alpha_0 - \theta_A \\ 0 & 0 & 0 & \lambda\cos 2\alpha_0 & 0 & 0 \\ 1-\theta_C & 0 & 0 & -3\lambda_C \cos 2\alpha_0 & -\theta_C - 3\lambda_C \sin^2\alpha & -3\lambda_C \sin\alpha_0 \cos\alpha_0 \\ & & & 0_{3x6} & & \end{pmatrix}.$$

The monodromy matrix was found numerically for equations (2.5). Dynamical system parameters are inherited from Fig. 1 and 2 (including the search for parameters λ and μ). Maximum characteristic multipliers of the monodromy matrix are depicted in Fig. 4.
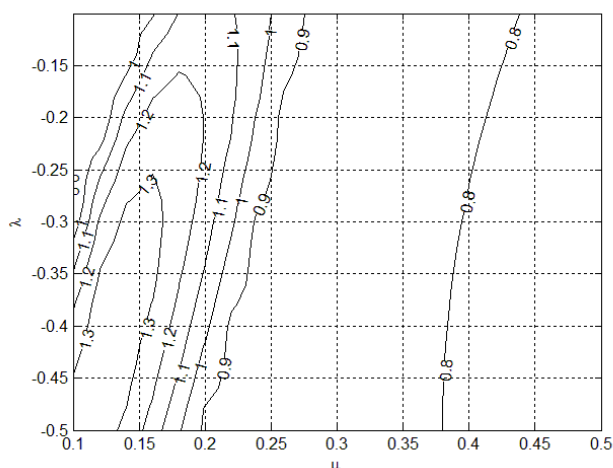
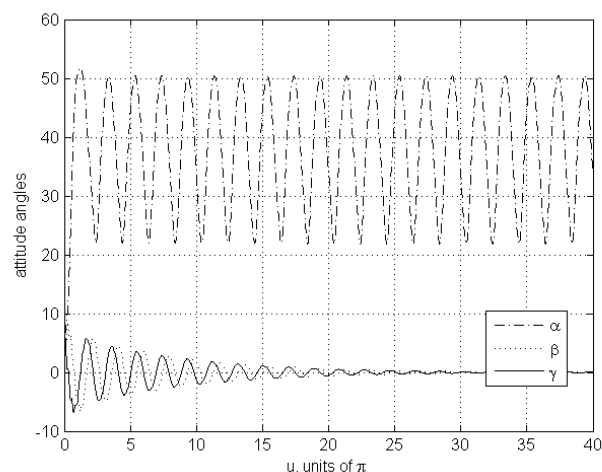Fig. 4. Planar periodical solutions stability

Fig. 5. Oscillations amplitude growth

Fig. 4 shows instability for small control torque (left part of the figure). Gravity introduces too large disturbance. Logically small gravitational torque (upper left corner) doesn't prevent stability. Outright numerical simulation of equation (2.1) provides slightly more optimistic results. Periodical motion exists even in the unstable area (Fig. 4). However oscillations amplitude may become unacceptably large (up to 60 degrees). These oscillations cannot be covered with approximate equations (2.4) that were obtained assuming small amplitudes. Hence large amplitude in initial equations corresponds to the instability in approximate equations. It's also important to note that motion remains planar even for the unstable exponents in fig. 4 (equation (2.1) is valid for the polar orbit regardless of any parameters). So generally speaking only approximate equations (2.4) experience qualitative changes. Initial equations are prone to quantitative changes as system parameters vary. This broadens the area of utility for results provided in fig. 1 and 2. Numerical analysis shows that it may be used for characteristic exponents up to approximately 1.1 (Fig. 4). Fig. 5 provides one example of numerical simulation with large oscillations amplitude (and characteristic exponent close to 1.1). This example utilizes parameters $\mu \approx 0.22$ and $\lambda \approx -0.176$ (the latter corresponds to $A = 1.4$ kg·m^2).

3.   Spatial motion on a circumpolar orbit

Consider the satellite moving on a circumpolar orbit. Solution of equations (1.6) is represented in the form

$$\mathbf{x} = \mathbf{x}_0 + \delta \mathbf{x}_1$$

where $\delta = \pi/2 - i$ is a small parameter, $\mathbf{x}_0$ is a generating solution (planar polar motion is used). The first order equations for $\mathbf{x}_1$ are

$$\dot{\mathbf{x}}_1 = \mathbf{A}(u)\mathbf{x}_1 + \mathbf{g}(u).$$

Matrix $\mathbf{A}$ is given in the previous section. Vector $\mathbf{g}$ is

$$\mathbf{g} = \begin{pmatrix} \varepsilon C/A\,\omega_{20} f_2 \\ 0 \\ -\varepsilon\omega_{20} f_1 + \varepsilon k_r g_2 f_1 \end{pmatrix}.$$

Equations that govern in-plane motion (variables $\alpha_{(1)}$, $\omega_{2(1)}$) are separated and has zero solution. Planar motion doesn't change in the first approximation. Out-of-plane oscillations (variables $\beta_{(1)}$, $\gamma_{(1)}$, $\omega_{3(1)}$, $\omega_{1(1)}$) are 2π-periodic due to the vector $\mathbf{g}$. Fig. 6 and 7 describe these periodical oscillations. Fig. 6 presents the amplitudes of the flywheel axis deviation from the orbit normal (orbit inclination 80 degrees). Fig. 7 provides initial phase φ_β of the angle β assuming that $\beta_{(1)} = A_\beta \sin(u + \varphi_\beta)$. Note that always $\varphi_\gamma - \varphi_\beta \approx \pi/2$ and with good confidence $\varphi_\beta \approx -\pi/4$. Fig. 6 and 7 are provided for the control torque typical values $\mu \geq 0.2$. This corresponds to the stable area of generating solution according to Fig. 4 (apart from the small unstable area where planar generating solution is still good enough).
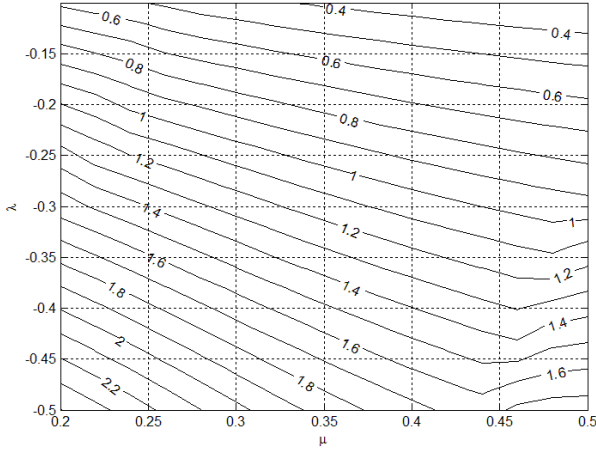

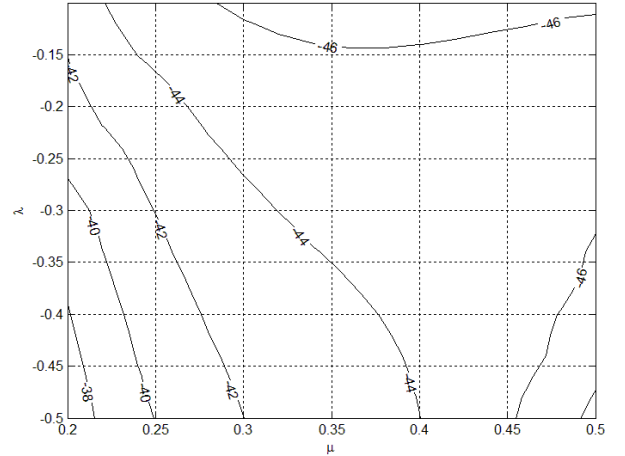Fig. 6. Amplitude of the flywheel axis deviation from the orbital normal

Fig. 7. Initial phase of angle β oscillations

Increase in parameter λ corresponds to the growth of the inertia moment A (it changes in the range 1.41-1.58 kg·m², two remaining inertia moments are unchanged). This in turn leads to the increase in parameter λ_C. As a result restoring gravitational torque out-of-plane influence is reduced. The flywheel axis deviation

from the orbit normal increases. As control torque raises this deviation reduces. One may assume this to be strange since the control torque disturbs out-of-plane attitude of the flywheel rotation axis. The observed effect is due to the damping control part acting together with the flywheel. The flywheel influence by far exceeds the disturbing out-of-plane influence of positional part of the control torque. Curiously this is not valid for large values of both control and gravitational torques. This is due to the lacking accuracy of generating planar periodical motion obtained in the previous section. Reverting to the specific example (A =1.5 kg·m^2, orbit inclination 80°), amplitudes of the attitude angles are $\delta\beta_{(1)}$ =1.51°, $\delta\gamma_{(1)}$ =1.31°. This provides the deviation of the flywheel axis from the orbit normal up to 1.29°. Numerical simulation (Fig. 8) provides maximum deviation 1.26°.
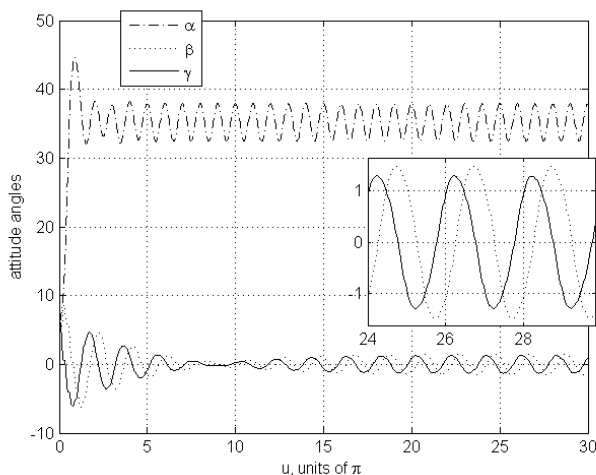

Fig. 8. Numerical simulation for circumpolar orbit

Numerical simulation was carried out with initial conditions 0.1 for each variable. Simulation of equations (1.2)-(1.3) shows that the results depicted in Fig. 6 are valid for almost every orbit excluding only the subequatorial ones. Fig. 6 corresponds to the orbit inclination 80 degrees (δ =10°). Orbit inclination 40° (δ =50°) leads to the amplitude of the flywheel axis deviation up to approximately 7.5°. This is about 6 times greater than 80° orbit provides. Linear dependence of the flywheel axis deviation from the orbit inclination is observed. Only δ is prone to change while $\mathbf{x}_1$ provided above is almost unchanged.

4. Planar motion on the orbit with inclination close to 45°

The latter pattern is due to the influence of the flywheel and damping control part. It is valid only for the out-of-plane motion. In-plane motion ensured with the control (1.5) persists only for the highly inclined orbits (approximately up to 50°).

Consider the subequatorial orbit. Steady state motion with the flywheel axis being almost parallel to the orbit normal leads to small first and third components of the geomagnetic induction vector in the bound reference frame. As a result the control torque acting in-plane (the second component of the torque) is small and cannot prevail over the gravitational torque. One may assume that the accuracy of in-plane stabilization degrades uniformly as the inclination decreases. However this is not the case. Accuracy drastically falls for orbit inclinations in the range 45-50°. This preliminary numerical simulations result should be treated analytically in order to find the border inclination leading to the sharp increase of the oscillations amplitude.

Consider the satellite moving on the orbit with inclination close to 45°, $i = \pi/4 + \delta$. Here δ is treated as a small parameter. The geomagnetic induction vector becomes

$$\mathbf{B} = B_0 \big/ \sqrt{2} \begin{pmatrix} \cos u \\ 1 \\ -2\sin u \end{pmatrix} + \delta B_0 \big/ \sqrt{2} \begin{pmatrix} \cos u \\ -1 \\ -2\sin u \end{pmatrix}.$$

Positional control part is two times less than on the polar orbit in linear approximation. Damping control part changes significantly. The in-plane damping control acquires dependence on the out-of-plane motion. In-plane motion analysis becomes too complicated. In order to separate out-of-plane motion note that it is found to be the small amplitude oscillations. Assume that

$$\beta = Am\sin(u - \pi/4), \; \gamma = Am\sin(u + \pi/4). \tag{4.1}$$

Here some additional assumptions were made. First the amplitudes of oscillations for both angles are equal to Am. This amplitude may be estimated using the previous section results taking into account that the amplitude rises proportionally to the inclination rise. This provides amplitudes on the 45° orbit to be approximately $A_\beta \approx 6.8°$, $A_\gamma \approx 5.9°$. Common amplitude Am is derived as a mean value. The initial phases according to the previous section are $\varphi_\beta \approx -44°$, $\varphi_\gamma \approx 49°$. However expressions (4.1) utilize values $\mp 45°$ for further analysis simplification. After all these assumptions in-plane motion is described with the equation

$$\ddot{\alpha} = m\sin\alpha\cos\alpha + \mu k_r \sin(\alpha_d - \alpha)\Big[(1+2\delta)(\cos u\sin\alpha - 2\sin u\cos\alpha)^2 +$$

$$+2Am\sin(u+\pi/4)(2\sin u\cos\alpha - \cos u\sin\alpha)\Big] - \underline{\mu(1+3\sin^2 u)\dot{\alpha}} -$$

$$-2\mu Am\dot{\alpha}\Big[\delta(1+3\sin^2 u) + \sin(u+\pi/4)(2\cos\alpha\sin u - \sin\alpha\cos u) +$$

$$+\sin(u-\pi/4)(2\sin\alpha\sin u + \cos\alpha\cos u +)\Big] +$$

$$+\mu Am\Big[\cos(u+\pi/4)(2\sin\alpha\sin u + \cos\alpha\cos u) -$$

$$\cos(u-\pi/4)(2\cos\alpha\sin u - \sin\alpha\cos u)\Big]. \tag{4.2}$$

The underlined part is analogous to (2.1). Ongoing analysis follows the scheme used in the section 2. Equations (4.2) are averaged assuming small control and gravitational torques. This provides the equilibrium position α'. Coefficients c_i found in the section 2 are slightly altered,

$$c_2' = c_2 - 1/4\, Am\mu(b+a)(\cos\pi/4 - 2\sin\pi/4) - 2Am\mu k_r(-\cos\pi/4\,a - 1/2\sin\pi/4\,b),$$

$$c_1' = c_1 + 1/2\, Am\mu(-a+b)(\cos\pi/4 - 2\sin\pi/4) - 2Am\mu k_r(\cos\pi/4\,b - 1/2\sin\pi/4\,a),$$

$$c_0' = c_0 + 1/2\, Am\mu(b+a)(\cos\pi/4 - 2\sin\pi/4).$$

Expressions for c_i obtained in the section 2 should also utilize $k_r' = k_r(1+2\delta)$ instead of k_r. The linearized equations of motion are

$$\ddot{x} + \varphi_2\dot{x} + \varphi_1 x + \varphi_0 = 0, \tag{4.3}$$

$$\varphi_2 = -f_2 - f_2', \ \varphi_1 = -f_1 - f_1', \ \varphi_0 = -f_0 - f_0',$$

$$f_2' = -2\delta(1+3\sin^2 u) - 2Am\sin(u+\pi/4)(-a\cos u + 2b\sin u) -$$

$$-2Am\sin(u-\pi/4)(b\cos u + 2a\sin u),$$

$$f_1' = Am\cos(u-\pi/4)(b\cos u + 2a\sin u) - Am\cos(u+\pi/4)(a\cos u - 2b\sin u) -$$

$$-2Amk_r\sin(u+\pi/4)\Big[c(-2a\sin u - b\cos u) + d(2b\sin u - a\cos u)\Big],$$

$$f_0' = -Am\cos(u-\pi/4)(-a\cos u + 2b\sin u) + Am\cos(u+\pi/4)(b\cos u + 2a\sin u) -$$

$$-2Amk_r\sin(u+\pi/4)c(2b\sin u - a\cos u).$$

Expressions for f_i can be found in the section 2 (control gain is replaced with $k_r' = k_r(1+2\delta)$). The linearized equations lose the stability when the initial equations witness sharp amplitude increase. Fig. 9 provides the characteristic multipliers of equations (4.3) with respect to the orbit inclination and out-of-plane oscillations amplitude. The latter is governed mainly by the flywheel parameters that do not affect equations (4.3).
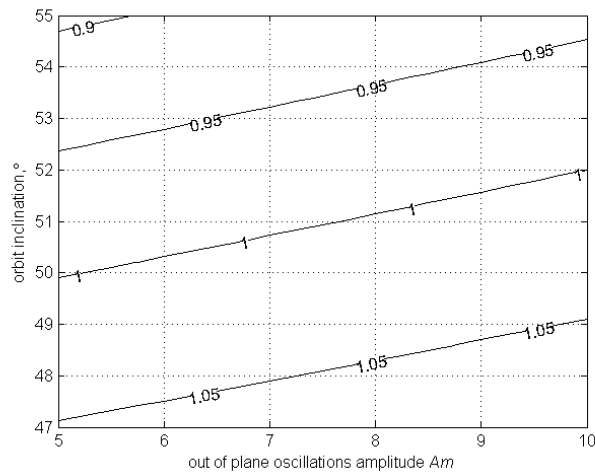
Fig. 9. Stability for orbit near *i*=45°

Fig. 9 shows the loss of stability for orbit inclination near 50-52°. The out-of-plane oscillations amplitude has negative effect on the stability. Fig. 10 and 11 provide the numerical simulation results for equations (1.6) and orbit inclinations 50° and 40° respectively.
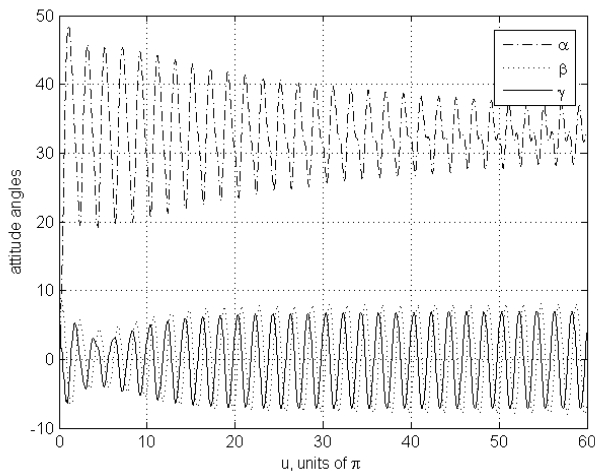

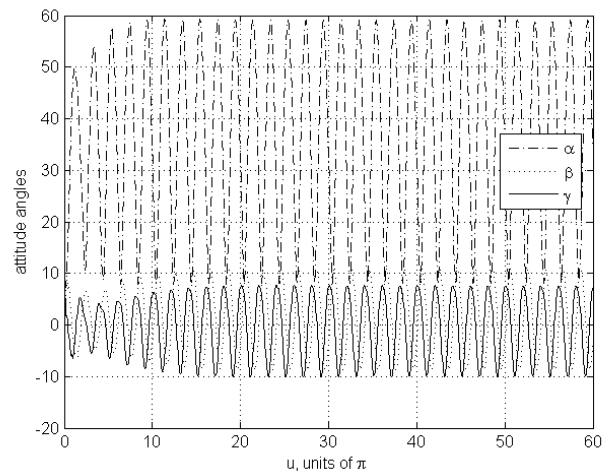Fig. 10. Numerical simulation of the initial linearized equations, incl. 50°

Fig. 11. Numerical simulation of the initial linearized equations, incl. 40°

Fig. 10 witnesses amplitude decrease. However, this change is rather slow. This case corresponds to the boundary situation. Linear equations (4.3) has asymptotically stable periodical solution with the small degree of stability. Fig. 11 corresponds to the knowingly unstable case for equations (4.3). Numerical simulation provides the oscillations amplitude up to 25°. This clearly renders the linearization assumption incorrect. Fig. 12 and 13 provide analogous result for the numerical simulation of the

initial nonlinear equations(1.2)-(1.3). Here γ_{ii} are the angles between the corresponding axes of the orbital and bound reference frames.
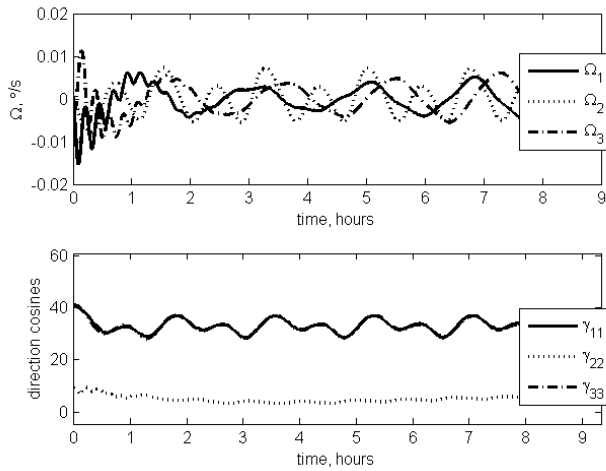

Fig. 12. Numerical simulation of the initial equations, inclination 50°

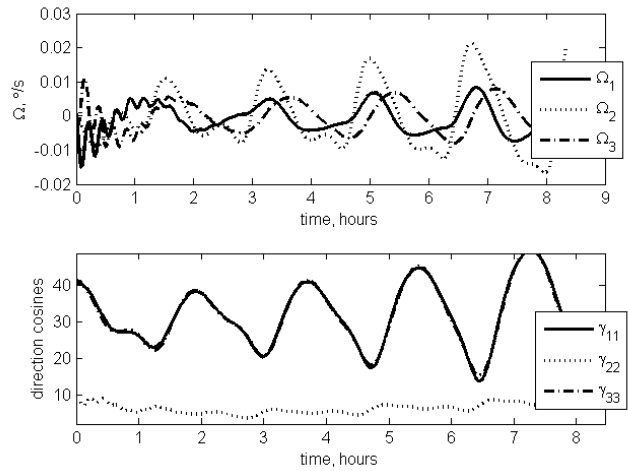Fig. 13. Numerical simulation of the initial equations, inclination 40°

Periodical motion can be seen in Fig. 12. However Fig. 13 clearly provides increase in the "amplitude" of oscillations. Fig. 14 brings the simulation results for the knowingly appropriate orbit.
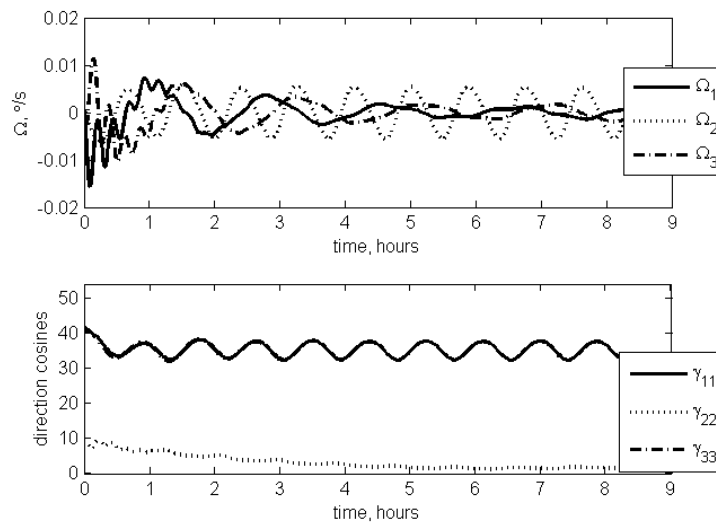

Fig. 14. Numerical simulation of the initial equations, inclination 70°

Numerical simulation of equations (1.6) shows amplitude decrease for subequatorial orbits. This is due to the geomagnetic induction vector being almost perpendicular to the orbit plane. As a result control (1.5) has negligible impact on the in-plane motion (orbit inclination becomes a small parameter). The satellite moves in the gravitational field with the small damping torque. The oscillations amplitude

decreases for inclinations near 20-25°. One may assume that control (1.5) is still strong enough to notably shift the equilibrium position. So the control is available to some extent in the narrow inclinations range. Control efficiency is debatable however since the satellite is closer to the gravitationally stably position than to the necessary position. On top of that simulation of the initial equations (1.2)-(1.3) further narrows the inclinations range. This range and corresponding motion is of little interest and may only be considered as a backup measure for some subequatorial satellites.

Conclusion

The satellite equipped with an active magnetic control system and a flywheel is considered. The control is proposed to ensure the necessary attitude of the satellite in the orbit plane. Motion in the vicinity of necessary attitude is assessed. Periodical solutions are found for planar and spatial motion on polar and circumpolar orbits. Stability analysis is provided. Sharp amplitude increase is verified for orbits near 45°. Numerical simulation cases are provided.

References

1. Ovchinnikov M.Y., Roldugin D.S. Dual-spin satellite motion in magnetic and gravitational fields // Keldysh Institute Preprints. 2015. № 22. 20 p.
2. Ovchinnikov M.Y. et al. Motion of a Satellite Equipped with a Pitch Flywheel and Magnetic Coils in Gravitational Field // Cosmic Research. 2017. V. 55, № 3. pp. 207–213.
3. Pichuzhkina A.V., Roldugin D.S. Geomagnetic field models for satellite angular motion // Keldysh Institute Preprints. 2016. № 87. 25 p.
4. Malkin I.G. Some problems in the theory of nonlinear oscillations. Oak Ridge: U.S. Atomic Energy Commission, Technical Information Service, 1959. 589 p.